

Time-ordering effects in K -shell excitation of 170-MeV Ne^{7+} colliding with gas atoms: Double excitation

N. Stolterfoht, A. Mattis, D. Schneider,* G. Schiwietz, and B. Skogvall†

Hahn-Meitner-Institut Berlin GmbH, Bereich Festkörperphysik, Glienickerstrasse 100, D-14 109 Berlin, Federal Republic of Germany

B. Sulik and S. Ricz

Institute of Nuclear Research, Bem tér 18c, H-4001 Debrecen PF 51, Hungary

(Received 24 June 1994)

The method of 0° Auger spectroscopy was utilized to measure state-selective K -shell excitation in Li-like Ne^{7+} incident with 170-MeV on H_2 , He, CH_4 , Ne, and Ar. Interferences between first- and second-order mechanisms are searched for in the production of the doubly excited states $1s2p^2D$ and $1s2p^2S$. The semiclassical approximation is applied to study time ordering of the double-excitation process. It is shown that time ordering is lost for the second-order amplitude so that it is unable to interfere with the first-order amplitude. The doubly excited state $1s2p^2S$ is predominantly produced by the single-electron transition $1s \rightarrow 2s$ followed by configuration interaction with $1s2s^2S$. Discrepancies occur between theory and experiments as the state $1s2p^2D$ is interpreted in terms of the independent dipole transitions $1s \rightarrow 2p$ and $2s \rightarrow 2p$.

PACS number(s): 34.50.Fa

I. INTRODUCTION

In recent years, energetic ion-atom collisions have received particular attention with regard to dynamic electron-correlation effects [1–3]. They are produced by the residual electron-electron interaction not incorporated in the independent-particle model (IPM) [4]. This residual interaction, also denoted dielectronic interaction [5], is represented by two-body operators. The major part of the electron-electron interaction is treated as a mean field which may be considered as the monoelectronic aspect of the electron-electron interaction. In the framework of atomic structure theory, the Hartree-Fock method is used to describe the mean-field part of the electron-electron interaction. Accordingly, the dielectronic part is identified as the difference between the exact and the Hartree-Fock solution.

In ion-atom collisions, the border line between the monoelectronic and dielectronic aspects is not easy to draw. In a dynamic collision system, the electronic mean field is time dependent. In general, it is difficult to distinguish between dynamic mean-field effects and electron correlation. To avoid these difficulties, attempts were made to retain static mean fields by using the independent-particle model with frozen orbitals (IPM-FO) [6]. Consequently, shake processes, produced by the change of the mean field, are considered as phenomena occurring beyond the IPM. Also, the Pauli exclusion principle, which is generally incorporated in the station-

ary Hartree-Fock method, has been considered to produce dynamic electron correlation referred to as Pauli correlation [7,8]. Thus the concepts concerning electron-correlation phenomena in ion-atom collisions are still controversial and their clarification needs further effort.

Detailed information about the collision mechanisms may be obtained from interference effects produced by the interplay of first- and second-order mechanisms. In the past, particular effort has been devoted to experiments concerning double ionization of He by fast ions [1]. In this case, an interference between the two-step process TS-1 involving *one* nucleus-electron interaction followed by an electron-electron interaction and the two-step process TS-2 involving *two* nucleus-electron interactions has been studied [9,10]. In lowest order the amplitudes for TS-1 is proportional to the projectile charge Z_p whereas the amplitude for TS-2 is proportional to Z_p^2 . Therefore, an interference term is produced depending on Z_p^3 and, hence, on the sign of Z_p . Similar interference effects have been considered in the process of double excitation [11] and they have been searched for experimentally [12,13].

Recently, McGuire and Straton [14] have pointed out the correspondence between interference and time ordering in second- or higher-order events. Time ordering is a fundamental phenomenon in time-dependent perturbation theory [15] which, in turn, constitutes the basis of the semiclassical approximation (SCA) [16,17]. McGuire and Straton [14] have shown for rather general cases that time ordering in a two-step process is a necessary condition for interference effects. Similar conclusions have been drawn by Briggs and Macek [18] who showed by time-reversal argument that interferences between first- and second-order events cancel in the case of double excitation.

A two-step process is ordered in time, if the first step

*Present address: Lawrence Livermore Laboratory, P.O. Box 808, Livermore, CA 94550.

†Present address: Technische Universität Berlin, Institut für Strahlungs- und Kernphysik, D-1000 Berlin, Germany.

has to occur before the second one can take place. It should be emphasized that the two-step processes TS-1 and TS-2 provide obvious examples for the phenomenon of time ordering. The TS-1 process involves a mono-electronic process produced by ion-electron interaction, which is required before the dielectronic process due to the electron-electron interaction can take place. Hence, in this case, time ordering is essential. However, TS-2 consists of two mono-electronic processes where time ordering is lost when the action of one electron takes place independent of the other one.

In two recent papers [19,20], hereafter referred to as (I) and (II), respectively, theoretical and experimental work concerning time ordering has been performed. In (I) the basic formalism of time-ordered two-step processes has been given. It has been shown that time ordering is lost in the independent-particle frozen-orbital model, where the action of one electron may take place before or after the action of the other electron. Formally it is shown that the loss of time ordering is due to a combination of two associated excitation paths. The new point of the theoretical analysis concerns the disappearance of interference effects. As the time ordering is lost, interferences between first- and second-order terms are canceled.

To verify the theoretical predictions, time-ordering effects were studied experimentally using the method of 0° Auger spectroscopy. In (II) the attention is focused on the mechanisms for *single* excitation. Time ordering has been regained because of a Pauli blocking mechanism and interferences between first- and second-order terms have been observed in agreement with calculations using the SCA. Besides the single-excitation data studied in (II), the experimental results contain information about the process of *double* excitation. This latter process will be considered here.

In this work, time-ordering and interference effects are studied for the processes of double excitation in 170-MeV Ne^{7+} colliding with different target atoms. The high incident energy is chosen to insure that second-order effects are small, although, still observable. However, third- and higher-order terms are likely to become negligible. At these high energies, the attempt is made to search for interference effects in the production of doubly excited states, associated with the *K*-shell excitation of Ne^{7+} . In

Sec II the principles of the present method are discussed and brief information about the experiment is given. In Sec. III, the time ordering of the present two-step processes is verified. For the TS-2 process, time ordering is found to be lost. In Sec. IV, the experimental data are compared with the SCA calculations. In particular, the experiment is analyzed in view of the predicted losses of time ordering and the corresponding interferences effects.

II. GENERAL CONSIDERATIONS AND EXPERIMENT

The principles of double excitation of Ne^{7+} are discussed by means of Fig. 1 which depicts the final states with the dominant components $1s2s^2S$, $1s2p^2S$, and $1s2p^2D$. Different conventions are used to denote the final states. In brief, these states are labeled *c*, *d*, and *e* as shown in Table I. If no conflict is possible, each state is specified by its dominant component although it may involve further significant components. Due to configuration interaction, the components $1s2s^2S$ and $1s2p^2S$ are strongly mixed. To distinguish the mixed states from their dominant component, the additional labels are used, such as $1s2s^2_cS$, and $1s2p^2_dS$. Hence, electron-correlation phenomena play an important role in the 2S states, restricting the applicability of the IPM for the final states.

Unlike the two 2S states, the final state $1s2p^2D$ cannot find a partner for configuration mixing within the $n=2$ manifold. The same is true for the intermediate states $1s^22p^2P$ and $1s2s2p^2P$. (The two-step processes, treated in Paper (II), are disregarded as they would contribute here in third order). Since the interaction with configurations involving the manifold $n \geq 3$ is neglected, the intermediate states retain single-configuration states. Hence, in practice, it is assumed that the IPM is valid during the collision.

From Fig. 1 it is seen that the single-configuration state $1s2p^2D$ is uniquely excited by the two-step process composed of the two dipole transitions $1s \rightarrow 2p$ and $2s \rightarrow 2p$. Hence, the state $1s2p^2D$ may be used to study exclusively this two-step process. On the contrary, the multiconfiguration state $1s2p^2_dS$ is also excited by a *one-step* process. This is due to the fact that the $1s2p^2_dS$ state involves, besides its dominant component, also the

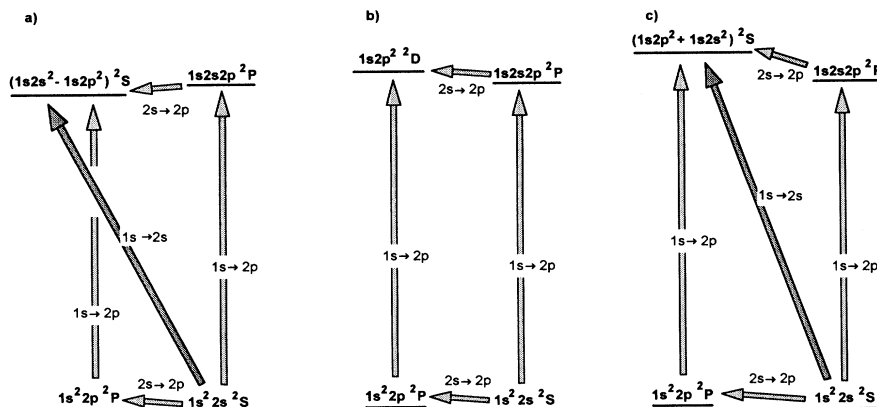


FIG. 1. Diagrams indicating mechanisms for double excitation of a Li-like system. In (a) and (c) are shown the interplay of the single monopole transition $1s \rightarrow 2s$ with the pair of dipole transitions $1s \rightarrow 2p$ and $2s \rightarrow 2p$ leading to states which are affected by configuration interaction. Diagram (b) exhibits a case limited to the dipole transitions.

TABLE I. Labels used to abbreviate paths with intermediate states, dominant components in the final states, and final states used in the present equations.

Path with intermediate state	Dominant component of the final state	Final state
$k: 1s2s2p^2P$	$q: 1s2s^2S$	$c: 1s2s^2S$
$\bar{k}: 1s^22p^2P$	$p: 1s2p^2S$ $1s2p^2D$	$d: 1s2p^2S$ $e: 1s2p^2D$

admixture $1s2s^2S$ which is created by the single transition $1s \rightarrow 2s$. Moreover, as seen from Fig. 1, the $1s2s^2S$ state contains, besides its dominant component, the admixture $1s2p^2S$. Hence, the first- and second-order processes lead to different components in the final state which ought to be added coherently. Thus, in principle, interference effects are possible in both cases. It should be added that the single $1s \rightarrow 2s$ transition followed by configuration interaction corresponds to the TS-1 mechanism, whereas the pair of dipole transitions $1s \rightarrow 2p$ and $2s \rightarrow 2p$ corresponds to the TS-2 mechanism [10], mentioned earlier. In the following, the possibilities for interferences between these mechanisms are analyzed theoretically and experimentally.

The experiments are concerned with Auger electron emission from fast Li-like ions Ne^{7+} which are excited by different target atoms. Hence, the collision system is inverted, i.e., the K electron of the highly ionized projectile is transferred to a bound state by interaction with a neutral target atom. The K -shell excitation is followed by Auger transitions ejecting monoenergetic electrons. These electrons were measured with high resolution using the method of 0° Auger spectroscopy [21–25]. The experiments were performed at the VICKSI accelerator facility of the Hahn-Meitner Institut Berlin. The experimental setup has been described in (II) so that no further details shall be given here.

The measurements yielded high-resolution K Auger electron spectra of Ne^{7+} composed of well separated lines [see Fig. 2 in (II)]. Individual lines were attributed to the double-excitation states discussed above. A fitting procedure by Gaussians was used to determine the line intensities. Hence, quantities are obtained that are propor-

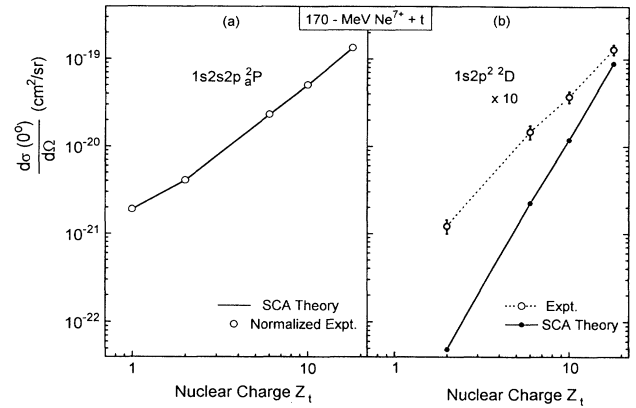


FIG. 2. Differential cross section $d\sigma(0^\circ)/d\Omega$ for Auger electron emission at 0° from 170-MeV Ne^{7+} colliding with H_2 , He , CH_4 , Ne , and Ar as a function of the target nuclear charge Z_t . The left-hand figure shows experimental data for the state $1s2s2p^2P$ which are normalized to theoretical results obtained from semiclassical calculations (see also Table IV). The right-hand figure shows a comparison of experimental and theoretical data for the state $1s2s^2S$.

tional to the differential cross section $d\sigma(0^\circ)/d\Omega$ for Auger emission at 0° .

Finally, the experimental data were put on an absolute scale using theoretical results for normalization. In Paper (II), differential cross sections $d\sigma(0^\circ)/d\Omega$ for the emission of Auger electrons at an angle of 0° have been evaluated for the single-excitation state $1s2s2p^2P$. The theoretical method will be outlined further below. The theoretical results imply the Auger yields from the work by Chen [26]. It is noted that the Auger yield, associated with the decay of the $1s2s2p^2P$ state, deviate significantly from unity. The theoretical results of the state $1s2s2p^2P$ were used to normalize the experimental data as shown in Fig. 2(a). In Table II, the final experimental data are given. After normalization by the reference state $1s2s2p^2P$, a comparison between absolute experimental and theoretical data can be carried out for the other states. This shall be done in the next sections.

TABLE II. Differential cross sections for Auger emission at 0° . The data are obtained from the experimental results in (II) after normalization of the $1s2s2p^2P$ data to theoretical cross sections. The experimental data for H_2 are normalized to theoretical results for H .

Target gas	$1s2s^2S$ (cm^2/sr)	$1s2s2p^2P$ (cm^2/sr)	$1s2s2p^2P$ (cm^2/sr)	$1s2p^2D$ (cm^2/sr)	$1s2p^2S$ (cm^2/sr)
H	2.62×10^{-22}	$1.90 \times 10^{-21*}$	5.7×10^{-22}		
He	7.19×10^{-22}	$4.08 \times 10^{-21*}$	1.11×10^{-21}	1.2×10^{-22}	5.5×10^{-23}
CH_4	3.5×10^{-21}	$2.32 \times 10^{-20*}$	6.5×10^{-21}	1.5×10^{-21}	4.9×10^{-22}
Ne	9.4×10^{-21}	$5.04 \times 10^{-20*}$	1.15×10^{-20}	3.7×10^{-21}	2.24×10^{-21}
Ar	2.07×10^{-20}	$1.35 \times 10^{-19*}$	2.87×10^{-20}	1.3×10^{-20}	8.1×10^{-21}

*Normalized to theoretical cross sections.

III. ANALYSIS OF TIME ORDERING

A. Theoretical method

To treat time ordering, we recall a few equations from the earlier Paper (I). In the SCA, the first-order amplitude is given by [15]

$$A_{if}^{(1)} = -i \int_{-\infty}^{\infty} d\tau V_{if}(\tau) e^{-i\omega_{if}\tau}, \quad (1)$$

where $\omega_{if} = E_f^a - E_i^a$ are transition energies and V_{if} are the corresponding coupling matrix elements. As shown in Table III, the first-order amplitude $A_{if}^{(1)}$ is either real or imaginary depending on the odd or even symmetry of the interaction matrix element V_{if} .

In contrast to the first-order amplitude, the corresponding second-order amplitude has both real and imaginary contributions. An individual second-order amplitude is obtained as

$$A_{if}^k = - \int_{-\infty}^{\infty} d\tau V_{kf}(\tau) e^{-i\omega_{kf}\tau} \times \int_{-\infty}^{\tau} d\tau' V_{ik}(\tau') e^{-i\omega_{ik}\tau'}. \quad (2)$$

The quantity A_{if}^k is referred to as *time-ordered* amplitude. The corresponding *double-path amplitude* $A_{if}^{k\bar{k}}$ is obtained by combining the associated paths k and \bar{k}

$$A_{if}^{k\bar{k}} = A_{if}^k + A_{if}^{\bar{k}}, \quad (3)$$

where the path \bar{k} is formed by time inversion of the two-step process involved in path k .

The quantity $A_{if}^{k\bar{k}}$ is referred to as *non-time-ordered amplitude*, if it can be expressed in terms of a product of single-electron amplitudes representing the underlying one-electron events of the two-step process. In (I) it has formally been shown that the loss of time ordering is based on the validity of the IPM-FO which, in turn, is based on ‘‘frozen’’ energies and orbitals [see Eqs. (16) and (17) in (I), respectively]. It should be kept in mind, however, that the validity of the IPM-FO is not a necessary condition for the loss of time ordering. The loss of time ordering will be discussed in detail further below.

The single-electron amplitudes for the excitation of the Ne^{7+} projectile were calculated numerically using hydrogenic wave functions. These wave functions are expected

to be adequate for the description of the highly charged projectile Ne^{7+} . It is recalled that the collision system is inverted. Hence, the projectile is excited by neutral target particles whose nuclear charge is significantly screened. As in (II) particular effort was devoted to the adequate treatment of the screening effects by neutral target atoms. The screening effects were calculated using the methods recently developed by Ricz *et al.* [27].

Besides the mono-electronic contribution by the screened nucleus, the dielectronic contribution from the interacting target and projectile electrons was taken into account in the excitation probabilities. It was determined using methods similar to those given by Montenegro and Meyerhof [28]. As in (II) it is found that the influence of the dielectronic part is significant for the light targets H_2 and He, whereas it becomes negligible for the heavier targets Ne and Ar.

B. Loss of time ordering

In the present collision system, the conditions of frozen energies and orbitals are not fulfilled. Hence, it was an important matter of the present analysis to verify whether the time ordering is lost for the double-path amplitude $A_{if}^{k\bar{k}}$ that is obtained by combining the pair of associated paths A_{if}^k and $A_{if}^{\bar{k}}$. As noted before, these paths are formed by the dipole transitions $1s \rightarrow 2p$ and $2s \rightarrow 2p$ proceeding via the intermediate states $1s2s2p^2P$ and $1s^22p^2P$ (Fig. 1). It is seen that the associated energies differ significantly, e.g., the $2s - 2p$ energy differences in the paths leading to the state $1s2s^2S$ differ even in sign. Thus, we performed auxiliary calculations of the time-ordered amplitudes with exact energies in comparison with calculations of the non-time-ordered amplitude assuming frozen orbitals [see Eq. (16) in (I)].

Examples for the verification of time-ordering effects are shown in Tables IV and V comparing results for frozen and relaxed orbitals. The cases refer to the excitation of the state $1s2p^2D$ with $M=0$ in collisions of 170-MeV Ne^{7+} on He. Calculations were made for a typical impact parameter of 0.2 a.u. The double excitation state $1s2p^2D$ is created by the transitions $1s \rightarrow 2pm_1$ and $2s \rightarrow 2pm_2$, where the pair of quantum numbers (m_1, m_2) is either equal to $(0,0)$ or $(\pm 1, \mp 1)$. [The latter notation represents both $(1, -1)$ and $(-1, 1)$.] The transition energies for relaxed orbitals (Table IV) are obtained from energy differences of multielectron states tabulated by Goett, Douglas, and Sampson [29]. The calculations were made for single-configuration states. For instance, the transition energy $\omega(1s \rightarrow 2p)$ was evaluated as $E(1s2s2p^2P) - E(1s^22s^2S)$ for path k , whereas it was identified with $E(1s2p^2D) - E(1s^22p^2P)$ for path \bar{k} . Analogously the transition energy $\omega(2s \rightarrow 2p)$ was determined. Finally, the frozen-orbital energies were chosen as mean values of the corresponding relaxed orbitals.

It is seen from Table V that the double-path amplitudes $A_{if}^{k\bar{k}}$ for the *frozen* orbitals are real in accordance with the results in Table III. The time-ordered amplitudes A_{if}^k and $A_{if}^{\bar{k}}$ imply large imaginary contributions equal in absolute value but opposite sign so that they are canceled as the associated amplitudes are summed, i.e., as

TABLE III. Even or odd symmetry of the matrix elements V_{if} produced by the interaction V . In parentheses are also given the real or imaginary value of the corresponding transition amplitude $A_{if}^{(1)}$. The quantity $\Delta\Pi$ denotes the change of parity and ΔM denotes the change of magnetic quantum number in the transition from the initial to the final state.

Transition	$\Delta\Pi$	$\Delta M = 0$	$\Delta M = 1$	$\Delta M = 2$
Monopole	no	even (imaginary)		
Dipole	yes	odd (real)	even (imaginary)	
Quadrupole	no	even (imaginary)	odd (real)	even (imaginary)

TABLE IV. Energies ω_{if} for the transition $1s \rightarrow 2p$ and $2s \rightarrow 2p$ in Ne^{7+} and the corresponding effective charge Z_{eff} used for scaled hydrogenic wave functions. For relaxed orbitals, the transition energy $\omega(1s \rightarrow 2p)$ was set to be equal to $E(1s2s2p^2P) - E(1s^22s^2S)$ for path k with the intermediate state $1s2s2p^2P$, whereas it was identified with $E(1s2p^2D) - E(1s^22p^2P)$ for path \bar{k} with the intermediate state $1s^22p^2P$. Analogously, the transition energy $\omega(2s \rightarrow 2p)$ was identified with $E(1s2p^2D) - E(1s2s2p^2P)$ for path k and $E(1s^22p^2P) - E(1s^22s^2S)$ for path \bar{k} . The frozen-orbital energies were chosen as mean values of the corresponding relaxed orbitals.

Orbital	Path	ω_{if}		Z_{eff}	
		$1s \rightarrow 2p$ (a.u.)	$2s \rightarrow 2p$ (a.u.)	$1s \rightarrow 2p$	$2s \rightarrow 2p$
Frozen	k :	33.28	0.585	9.233	9.233
	\bar{k}	33.28	0.585	9.233	9.233
Relaxed	k :	33.42	0.45	9.233	9.233
	\bar{k}	33.16	0.72	9.233	9.233

the double-path amplitude $A_{if}^{k\bar{k}}$ is formed. On the contrary, the imaginary amplitudes for *relaxed* orbitals are slightly different in the absolute value so that an imaginary contribution remains in the double-path amplitude $A_{if}^{k\bar{k}}$. However, these imaginary contributions are relatively small so that they do not play an essential role. It should be noted for the present examples that the coupling matrix elements were kept constant when going from frozen to relaxed orbitals. Table IV indicates that the same effective charge Z_{eff} of the projectile was used for all transitions.

Additional calculations were performed in changing also the coupling matrix elements. This was done by varying the effective charge Z_{eff} within the range of about one unit. We realize that such calculations involve problems due to the nonorthogonality of the related wave functions. Therefore, we shall not present further details.

TABLE V. Time-ordered amplitudes A_{if}^k and $A_{if}^{\bar{k}}$ for the paths k and \bar{k} , respectively, and double-path amplitudes $A_{if}^{k\bar{k}}$ for the two-step process ($1s \rightarrow 2pm_1$, $2s \rightarrow 2pm_2$) producing the final state $1s2p^2D$ with $M=0$ in 170-MeV Ne^{7+} colliding with He. The impact parameter is $b=0.2$ a.u. The amplitudes refer to $(m_1, m_2) = (0, 0)$ and $(\pm 1, \mp 1)$.

Orbital	Amplitude	(0,0)		($\pm 1, \mp 1$)	
		Real (10^{-5})	Imaginary (10^{-5})	Real (10^{-5})	Imaginary (10^{-5})
Frozen	A_{if}^k	-1.507	46.43	32.4	-5.470
	$A_{if}^{\bar{k}}$	-1.507	-46.43	32.4	5.470
	$A_{if}^{k\bar{k}}$	-3.01	0	64.8	0
Relaxed	A_{if}^k	-1.167	46.61	32.4	-5.568
	$A_{if}^{\bar{k}}$	-1.846	-46.25	32.5	5.374
	$A_{if}^{k\bar{k}}$	-3.01	0.36	64.9	-0.194

With some caution, however, it is concluded that the change of the coupling matrix elements indicated only small effects on the double-path amplitudes. This shows that time-ordering effects do not play a significant role neither for the absolute cross sections nor for the interference effects considered further below. Hence, we conclude that the loss of time ordering in the excitation amplitude is likely to be a valid assumption for the present cases.

IV. COMPARISON BETWEEN THEORY AND EXPERIMENT

Since the time ordering is lost, the amplitude $A_{if}^{k\bar{k}}$ can be given as a linear combination of products of single-electron amplitudes representing the transitions $1s \rightarrow 2pm_1$ and $2s \rightarrow 2pm_2$. The coupling of the angular momentum pairs pm_1 and pm_2 of the individual electrons to the total angular momenta L and M of the final state $f(LM)$ is evaluated by means of Clebsch-Gordon coefficients

$$A_{if(LM)}^{k\bar{k}} = \sum_{m_1 m_2} \langle 11m_1 m_2 | LM \rangle a_{1s \rightarrow 2pm_1} a_{2s \rightarrow 2pm_2}, \quad (4)$$

where $a_{1s \rightarrow 2pm_1}$ and $a_{2s \rightarrow 2pm_2}$ are the single-electron amplitudes for the transitions $1s \rightarrow 2pm_1$ and $2s \rightarrow 2pm_2$, respectively.

The second-order amplitude $A_{if}^{k\bar{k}}$ from Eq. (4) is used to determine the corresponding excitation cross section for the final state f

$$\sigma_f = 2\pi \int_0^\infty |A_{if}^{k\bar{k}}|^2 b db. \quad (5)$$

This quantity may be compared with the experimental data. It is recalled that the second-order amplitude is expected to depend on the squared charge of the exciting target particle. Since the target nucleus is screened, it is useful to consider an effective target charge q_t . The evaluation of the excitation cross section σ_f allows for defining q_t by means of $\sigma_f = (q_t/Z_t)^2 \sigma_f^{\text{bare}}$ where σ_f^{bare} is the corresponding cross section for the bare target atom. For the present cases it is found that the values of q_t/Z_t range from 0.5–0.8 depending on the final state f , see also in (II). These values show that the screening effects are indeed significant. The effective target charge q_t will often be used instead of the atomic number Z_t to substantiate qualitative considerations in the following.

Excitation cross sections were calculated by means of Eq. (5) for the final states $1s2s^2S$, $1s2p^2D$, and $1s2p^2S$. In (II), similar calculations were carried out for the single-excitation state $1s2s2p^2P$ which was chosen as reference to normalize the experimental results [Table II and Fig. 2(a)]. It is recalled from (II) that the single-configuration state $1s2s2p^2P$ is strongly influenced by dealignment effects.

On the other hand, dealignment effects are found to be small for the states $1s2s^2S$, $1s2p^2D$, and $1s2p^2S$ considered in this work. Hence, in this case, transitions to the final magnetic quantum number $M=0$ are primarily treated, as the experimental data are obtained by observation of Auger electrons at 0° . Within the L - S coupling

scheme, only states with $M=0$ contribute at 0° , since the Auger transition leaves the ion in an S state [30]. Accordingly, the total cross section is multiplied by $(2L+1)/4\pi$, to obtain differential cross sections $d\sigma(0^\circ)/d\Omega$ for electron ejection at 0° .

To gain information about the production of the single-excitation state $1s2s^2S$, calculations were performed for the monopole transition $1s \rightarrow 2s$. It is recalled, that this state is significantly mixed with the component $1s2p^2S$ yielding the multiconfiguration state $1s2s^2S$ (Table I). Thus, an adequate description of the latter state requires also a second-order calculation. In the following, the single-configuration and multiconfiguration states will be treated separately.

A. The single-configuration state $1s2p^2D$

First, we consider the state $1s2p^2D$, hereafter labeled e (Table I). The related second-order amplitude is evaluated for $M=0$. From Eq. (4) it follows that

$$A_{ie(M=0)}^{k\bar{k}} = \frac{1}{3}a_{1s \rightarrow 2p1}a_{2s \rightarrow 2p-1} + \frac{2}{3}a_{1s \rightarrow 2p0}a_{2s \rightarrow 2p0}. \quad (6)$$

For the transition $2s \rightarrow 2pm$ it is found that the population of the magnetic quantum numbers is not statistical, i.e., the occupation probability for the $m = \pm 1$ states is much larger than that for $m=0$ (see also Table V). Hence, in Eq. (6) the first term is dominant. The resulting amplitude was used to evaluate the total cross section from Eq. (5).

In Fig. 2(b) the results of the differential cross section calculations are compared with the experimental data. Good agreement is achieved only for the heaviest target Ar, whereas, considerable discrepancies between theory and experiment occur for the light target atoms H_2 and He. For the double-excitation state $1s2p^2D$ we expect a q_t^4 dependence of the production cross section where q_t is the effective target charge discussed above. Indeed, the theoretical data are found to be governed by a q_t^4 dependence [Fig. 2(b)]. However, comparison with Fig. 2(a) indicates that the variation of the experimental cross sections for the double-excitation state $1s2p^2D$ is similar to that for the single-excitation state $1s2s2p^2P$ which is expected to be proportional to q_t^2 . At present, we have no definite explanation for this finding. The disagreement between theory and experiment suggests that an essential aspect is still missing in the interpretation of the $1s2p^2D$ state.

Various effects may be considered to explain the disagreement between experiment and theory. We would not expect that the approximation of using hydrogenic wave function produces the large discrepancies observed between theory and experiment. Rather, it may be possible that the limitation of configuration interaction within the $n=2$ manifold is invalid. It would be useful to analyze the influence of configuration interaction between the final state $1s2p^2D$ and the closest single excitation state $1s2s3d^2D$ within the $N=3$ manifold. In this case, it is possible that the final state $1s2p^2D$ is excited via a TS-1 process where the $1s2s3d^2D$ excitation is followed by electron-electron interaction. This would explain that the excitation function of the double-excitation state

$1s2p^2D$ is similar to that of the single-excitation state $1s2s2p^2P$. Such TS-1 process will be considered later for the double-excitation state $1s2p^2S$.

Furthermore, it should be considered that strong coupling effects between the $2s0$ and $2p0$ orbitals occur so that a treatment beyond first-order perturbation theory is required. The present calculations shows that in $2s0 \rightarrow 2p0$ transitions the population of the $2p0$ orbital is transiently rather strong at the distance of closest approach. This is not evident, as the asymptotic $2p0$ population is found to be small after the collision. The explanation of this seeming controversy is that the significant $2p0$ population by $2s0 \rightarrow 2p0$ transitions in the incoming part of the collision is nearly completely canceled by the inverse $2p0 \rightarrow 2s0$ transitions in the outgoing part of the collision.

It is important to note that this ‘‘symmetry’’ in the $2p0$ population and depopulation may be broken, when the effective charge of the exciting particle (i.e., the neutral target atom) changes during the collision. Such dynamic screening may occur as the target atom is excited or ionized by the projectile. Then, the $2p0$ depopulation by the $2p0 \rightarrow 2s0$ transitions is incomplete and a significant population of the $2p0$ may remain. From our calculations we would expect that this dynamic screening of the target atom plays a significant role for the double-excitation state $1s2p^2D$.

The discrepancies observed between the theoretical and experimental data of the single-configuration state $1s2p^2D$ shall not further be studied here. Such investigation shall be devoted to forthcoming work. In this article, the attention is focused on possible interference effects in the production of the multiconfiguration states.

B. The multiconfiguration states $1s2s^2S$ and $1s2p^2S$

In the following we search for interferences between one- and two-step processes involving electron correlation. In principle, information about these interferences may be provided from the excitation of the multiconfiguration states $1s2s^2S$ and $1s2p^2S$. The configuration mixing gives rise to the linear combinations

$$|1s2s^2S\rangle = C|1s2s^2S\rangle - c|1s2p^2S\rangle, \quad (7)$$

$$|1s2p^2S\rangle = C|1s2p^2S\rangle + c|1s2s^2S\rangle, \quad (8)$$

where C and c are the dominant and the subordinate coefficients, respectively. The expansion coefficients were determined by means of a Hartree-Fock program [31] yielding the values of $C=0.94$ and $c=0.33$. These numbers show that the configuration mixing is significant in the present case.

Hereafter, the single-configuration components $1s2s^2S$ and $1s2p^2S$ are labeled q and p , respectively (Table I). It is also recalled that the mixed states are abbreviated by c and d . In accordance with Eq. (5) the excitation cross sections for these state are obtained as

$$\sigma_c = 2\pi \int_0^\infty |CA_{iq}^{(1)} - cA_{ip}^{k\bar{k}}|^2 b db, \quad (9)$$

$$\sigma_d = 2\pi \int_0^\infty |CA_{ip}^{k\bar{k}} + cA_{iq}^{(1)}|^2 b db. \quad (10)$$

These equations show that interferences are possible in the double-excitation process. It follows that the interferences originate from the coherent superposition of first- and second-order amplitudes which are proportional to the effective charge q_t and the square of the effective charge q_t^2 , respectively.

The present analysis, however, indicates that interference effects between the first- and second-order terms are negligible. As shown in the preceding section, the double-excitation process involves a pair of associated paths for which time ordering is practically lost. Thus, the second-order amplitude becomes essentially real, as it involves two dipole transitions. On the contrary, the first-order amplitude, associated with the $1s \rightarrow 2s$ monopole transition, is imaginary (Table III). Therefore, in the present case, the first- and second-order amplitudes cannot interfere.

Consequently, the cross sections are given as a sum of two incoherent contributions due to first- and second-order terms

$$\sigma_c = 2\pi \int_0^\infty |CA_{iq}^{(1)}|^2 b db + 2\pi \int_0^\infty |cA_{ip}^{k\bar{k}}|^2 b db, \quad (11)$$

$$\sigma_d = 2\pi \int_0^\infty |CA_{ip}^{k\bar{k}}|^2 b db + 2\pi \int_0^\infty |cA_{iq}^{(1)}|^2 b db. \quad (12)$$

The first-order amplitude $A_{iq}^{(1)}$ is based on the single-electron transition $1s \rightarrow 2s$ which was calculated using methods mentioned before.

The second-order term $A_{ip}^{k\bar{k}}(M=0)$ can be expressed in terms of single-electron amplitudes following from Eq. (4) for $M=0$

$$A_{ip}^{k\bar{k}}(M=0) = \frac{2}{3}a_{1s \rightarrow 2p1}a_{2s \rightarrow 2p-1} + \frac{1}{3}a_{1s \rightarrow 2p0}a_{2s \rightarrow 2p0}. \quad (13)$$

As before, on the right-hand side, the first term is dominant (Table V). Also, the explicit calculations show that, in Eqs. (11) and (12), the second-order term is considerably smaller than the first-order term. Although at high collision energies, the monopole transition $1s \rightarrow 2s$ is not so strong, it turns out that the second-order amplitude is even smaller. [Recall from (I) that the loss of time ordering is accompanied by a significant reduction of the amplitude.]

Accordingly, in Eq. (11), the second-order term can be fully neglected, as it is weighted by the square of the small coefficient c . Therefore, the theoretical cross sections for the $1s2s^2 {}^2S$ state were based entirely on first-order calculations which were found to be in fair agreement with experiment [Fig. 3(a)]. It is seen from a comparison of Figs. 2(a) and 3(a) that the q_t dependence of the production cross section for the $1s2s^2 {}^2S$ state is similar to that of the state the single-excitation states $1s2s2p {}^2P$. For single-excitation states, the production cross section is expected to be proportional to q_t^2 , as noted before.

In Eq. (12), describing the production of the double-excitation state $1s2p^2 {}^2S$, the second-order term is weighted by the square of the dominant coefficient C so that it cannot be fully neglected. However, the second-order term plays a noticeable role only for the high values of Z_t associated with the heavier target atoms Ne and Ar. For the lighter target atoms, the first-order term is dom-

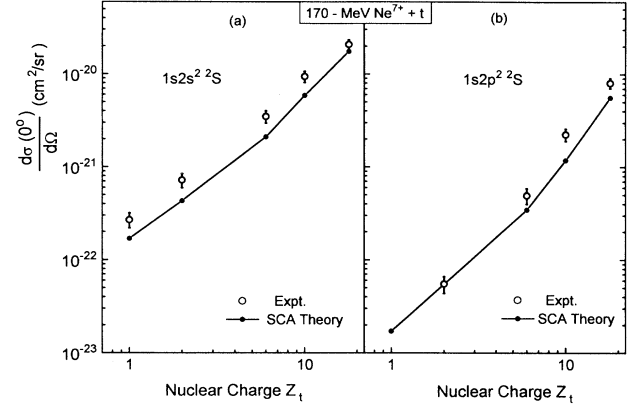


FIG. 3. Differential cross section $d\sigma(0^\circ)/d\Omega$ for Auger electron emission at 0° from 170-MeV Ne^{7+} colliding with H_2 , He, CH_4 , He, and Ar as a function of the target nuclear charge Z_t . In the left- and right-hand figures, experimental data are plotted for the state $1s2p^2 {}^2S$ and $1s2s^2 {}^2S$, respectively. The experimental data are compared with theoretical data obtained from calculations using the SCA.

inant. Nevertheless, since both first- and second-order processes are relevant, the excitation function for $1s2p^2 {}^2S$ varies with the effective target charge stronger than q_t^2 . This can be seen from Fig. 3(b) where the theoretical results are plotted in good agreement with the experimental data. Summarizing the foregoing discussion we point out that *double*-excitation of the state $1s2p^2 {}^2S$ is dominated by the TS-1 mechanism, i.e., by a *single*-electron transition followed by electron-correlation effects.

V. CONCLUDING REMARKS

In summary, time ordering and interference effects were studied for the process of double excitation in high-energy Ne^{7+} projectiles. The production mechanisms of the final single-configuration state $1s2p^2 {}^2D$ and the final multiconfiguration states $1s2s^2 {}^2S$ and $1s2p^2 {}^2S$ are analyzed. These states may be created by successive dipole transitions involving the intermediate states $1s^2 2p^2 {}^2P$ and $1s2s2p^2 {}^2P$, as well as by a single monopole transition process followed by electron-correlation effects. These mechanisms, similar to TS-1 and TS-2 [10], may interfere in the resulting excitation process.

To study these interference effects, the time ordering of the associated two-step processes is analyzed. Time ordering is a well-known phenomenon in time-dependent perturbation underlying the semiclassical approximation. Despite this long-standing knowledge, the concept of time ordering has scarcely been used in the field of energetic ion-atom collisions. In a previous paper, we have found that time ordering is required in the TS-2 mechanism as a necessary condition for the interference with TS-1. Similar results have previously been formulated by McGuire and Straton [14].

The theoretical analysis shows that time ordering is practically lost in the cases studied here so that interfer-

ence effects become negligible. In particular, the final state $1s2s^2{}_cS$ is produced uniquely by the $1s \rightarrow 2s$ monopole transition although this state contains a significant mixture of the $1s2p^2{}_cS$ component. Accordingly, for light target atoms, it is found that the double-excitation state $1s2p^2{}_cS$ is uniquely produced by TS-1 involving the production of the $1s2s^2{}_cS$ component by the $1s \rightarrow 2s$ transition, followed by strong configuration interaction. As expected for heavier targets, TS-2 plays an increasing role. Nevertheless, as interference effects are negligible, TS-1 and TS-2 add in an incoherent manner.

The theoretical treatment involves specific features. The collision system is inverted and strong screening effects are to be handled for the neutral target particles. The analysis includes various approximations, most of which are justified. A debatable assumption is the limitation of configuration interaction within the $n=2$ manifold. From this assumption it follows that the intermediate states $1s^22p^2P$ and $1s2s2p^2P$ are not affected by electron correlation and, thus, they remain single-configuration states. Hence, although electron correlation plays a role *after* the collision, it is not accounted for *during* the collision. The fact that electron correlation is missing during the collision may be the major reasons for the loss of time ordering in the TS-2 process. It has been

shown formally in (I) that time ordering is lost in the IPM-FO.

Alternatively, electron-correlation effects in the intermediate states could produce time ordering which, in turn, may produce interference effects. This finding may be accounted for in future work when interference effects are searched for. In particular, observations of interferences between TS-1 and TS-2 may be used as an indication that electron correlation occurs during the collision, a phenomenon also known as scattering correlation [1]. This would provide a method to study the dynamics of the breakdown of the IPM. Also the hypothesis of frozen orbitals may be verified during the collision. However, it is felt that the application of the time-ordering concept is still in its infancy. In the future, essential effort is needed to improve the knowledge about time ordering in ion-atom collisions.

ACKNOWLEDGMENTS

We are grateful to Jim McGuire for stimulating discussions concerning the concept of time ordering in ion-atom collisions. Thanks are devoted to Martin Grether and Ralf Köhrbrück for helpful comments on the manuscript.

-
- [1] J. H. McGuire, Phys. Rev. Lett. **49**, 1153 (1982); Nucl. Instrum. Methods Phys. Res. Sect. B **10**, 17 (1985); Phys. Rev. A **36**, 1114 (1987); *High-Energy Ion-Atom Collisions*, Vol. 294 of *Lecture Notes in Physics*, edited by D. Berényi and G. Hock (Springer-Verlag, Heidelberg, 1988), p. 415.
- [2] J. F. Reading and A. L. Ford, *Electronic and Atomic Collisions*, edited by H. B. Gilbody, W. R. Newell, F. H. Read, and A. C. Smith (North-Holland, Amsterdam, 1988), p. 693.
- [3] N. Stolterfoht, *Spectroscopy and Collisions of Few-Electron Ions*, edited by M. Ivascu, V. Florescu, and V. Zoran (World Scientific, Singapore, 1989), p. 342; Phys. Scr. **42**, 192 (1990).
- [4] A. Messiah, *Quantum Mechanics* (North-Holland, Amsterdam, 1970), Vol. II, p. 725.
- [5] N. Stolterfoht, Nucl. Instrum. Methods Phys. Res. Sect. B **53**, 477 (1991).
- [6] J. H. McGuire and L. Weaver, Phys. Rev. A **16**, 41 (1977).
- [7] J. Reading and A. L. Ford, Phys. Rev. A **21**, 124 (1980).
- [8] R. L. Becker, A. L. Ford and J. F. Reading, J. Phys. B **13**, 4059 (1980); R. L. Becker (private communication).
- [9] H. Knudsen, L. H. Andersen, P. Hvelplund, G. Astner, H. Cederquist, H. Danared, L. Liljeby, and K. G. Rensfelt, J. Phys. B **17**, 3545 (1984); H. Knudsen, L. H. Andersen, P. Hvelplund, J. Sørensen, and D. Ciric, *ibid.* **20**, L253 (1987).
- [10] L. H. Andersen, P. Hvelplund, H. Knudsen, S. P. Møller, K. Elsner, K. G. Rensfelt, and E. Uggeerhøj, Phys. Rev. Lett. **57**, 2147 (1986); L. H. Andersen, P. Hvelplund, H. Knudsen, S. P. Møller, A. H. Sørensen, K. Elsner, K. G. Rensfelt, and E. Uggeerhøj, Phys. Rev. A **36**, 3612 (1987).
- [11] J. H. McGuire and N. C. Deb, in *Atomic Physics with Positrons*, Vol. 169 of NATO Advanced Study Institute, Series B: Physics, edited by E. A. G. Armour and J. W. Hum-
bentson (Plenum, New York, 1988).
- [12] J. O. P. Pedersen and P. Hvelplund, Phys. Rev. Lett. **62**, 2373 (1989).
- [13] J. P. Giese, M. Schultz, J. K. Swenson, H. Schöne, M. Benhenni, S. L. Varghese, C. R. Vane, P. F. Dittner, S. M. Shafroth, and S. Datz, Phys. Rev. A **42**, 2131 (1990).
- [14] J. H. McGuire and J. C. Straton, Phys. Rev. A **43**, 5184 (1991).
- [15] A. Messiah, *Quantum Mechanics* (Ref. 4), p. 635.
- [16] M. R. C. McDowell and J. P. Coleman, *Introduction to the Theory of Ion-Atom Collisions* (North-Holland, Amsterdam, 1970), Chap. 4.
- [17] J. Bang and J. M. Hansteen, K. Dan. Vidensk. Selsk. Mat. Fys. Medd. **31**, 1 (1959).
- [18] J. S. Briggs and J. H. Macek, Adv. At. Mol. Opt. Phys. **28**, 1 (1991).
- [19] N. Stolterfoht, Phys. Rev. A **48**, 2980 (1993).
- [20] N. Stolterfoht, A. Mattis, D. Schneider, G. Schiwietz, B. Skogvall, B. Sulik, and S. Rizz, Phys. Rev. A **48**, 2986 (1993).
- [21] A. Itoh, T. Schneider, G. Schiwietz, Z. Roller, H. Platten, G. Nolte, D. Schneider, and N. Stolterfoht, J. Phys. B **16**, 3965 (1983); A. Itoh, D. Schneider, T. Schneider, T. J. Zouros, G. Nolte, G. Schiwietz, W. Zeitz, and N. Stolterfoht, Phys. Rev. A **31**, 684 (1985).
- [22] N. Stolterfoht, Phys. Rep. **146**, 315 (1987).
- [23] N. Stolterfoht, P. D. Miller, H. F. Krause, Y. Yamazaki, J. K. Swenson, R. Bruch, P. F. Dittner, P. L. Pepmiller, and S. Datz, Nucl. Instrum. Methods Phys. Res. Sect. B **24/25**, 168 (1987).
- [24] D. Schneider, N. Stolterfoht, G. Schiwietz, T. Schneider, W. Zeitz, R. Bruch, and K. T. Chung, Nucl. Instrum. Methods Phys. Res. Sect. B **24/25**, 173 (1987).
- [25] A. Mattis, Ph.D. thesis, Freie University, Berlin, 1990.

- [26] M. H. Chen, *At. Data Nucl. Data Tables* **34**, 301 (1986).
- [27] S. Ricz, B. Sulik, N. Stolterfoht, and I. Kádár, *Phys. Rev. A* **47**, 1930 (1993).
- [28] E. C. Montenegro and W. E. Meyerhof, *Phys. Rev. A* **46**, 5506 (1992).
- [29] A. Goett, F. Douglas, and P. Sampson, *At. Data Nucl. Data Tables* **29**, 535 (1983).
- [30] B. Cleff and W. Mehlhorn, *J. Phys. B* **7**, 593 (1974).
- [31] C. Froese Fisher, *Description of an Atomic Structure Software Package*, Department of Energy Report ER/10618-11, 1983 (unpublished).